A mode-selective circuit for TE_{01} gyrotron backward-wave oscillator with wide-tuning range

N. C. Chen, C. F. Yu, C. P. Yuan, and T. H. Chang[a)]
Department of Physics, National Tsing Hua University, Hsinchu 300, Taiwan

This study proposes a mode-selective circuit to suppress the competing modes in a TE_{01} gyrotron backward-wave oscillator (gyro-BWO). The circuit, also functioning as an interaction structure, comprises of several transverse slices. It eliminates the restrictions of the mode competitions and allows a longer interaction structure to optimize interacting efficiency. Mode-selective effect will be analyzed. Experimental results indicate that the *Ka*-band TE_{01} fundamental harmonic gyro-BWO is capable of continuous tuning from 31.4 to 36.4 GHz with a peak efficiency of 23.7%, corresponding to 100 kW at $I_b = 4.5$ A and $V_b = 93.6$ kV. © *2009 American Institute of Physics*.
[DOI: 10.1063/1.3097236]

A gyrotron backward-wave oscillator (gyro-BWO), based on the electron cyclotron maser, is a frequency-tunable, high-power, coherent millimeter-wave source. The properties of gyro-BWO have been theoretically studied[1,2] and experimentally demonstrated.[2–6] The continuous frequency tuning by varying the magnetic field or the beam voltage in a nonresonant structure has generally been evidenced with fundamental mode operation [rectangular TE_{10},[3] cylindrical TE_{11},[6] and helical corrugated TE_{-11}/TE_{21} (Refs. 4 and 5)]. As interest in the terahertz-wave regime grows, the operation of gyro-BWO in high-order mode is preferred due to the power-handling capability. The severe transverse mode competition arises because the separation between the cutoff frequencies of adjacent transverse modes decreases as the order of the mode increases.

Figure 1 plots the frequency-k_z diagrams of the 11 lowest TE modes and the fundamental ($s=1$) as well as second ($s=2$) cyclotron harmonic beam-wave resonance lines for a TE_{01} mode, fundamental harmonic, *Ka*-band gyro-BWO. Oscillation occurs at the intersection of the waveguide mode curve and the beam-wave resonance line. The beam-wave coupling strength for a transverse mode is strongly related to the electron guiding center r_c.[7] When r_c is set to the position of strongest coupling for the TE_{01} mode fundamental harmonic interaction (denoted as $TE_{01}^{(1)}$), the potential parasitic oscillations are $TE_{21}^{(1)}$, $TE_{31}^{(1)}$, $TE_{41}^{(1)}$, and $TE_{02}^{(2)}$. Based on the coupling strength, $TE_{21}^{(1)}$ and $TE_{31}^{(1)}$ modes are detrimental in the lower and higher magnetic tuning regions, respectively. The stable tuning region is shrunk greatly. The competing behaviors of TE_{01} gyrotrons have experimentally explored.[8]

To effectively suppress unwanted oscillations, several mode-selective circuits have been developed. A slotted structure was utilized on a TE_{31} third-harmonic gyrotron traveling wave tube (gyro-TWT) amplifier.[9] An axially sliced interaction circuit, which interrupts the wall current of the unfavorable mode, was developed for TE_{21} second harmonic gyro-TWT and provided a very high output power (207 kW at 15.7 GHz).[10] A helical corrugated structure, which changes the dispersion relation and operates with hybrid modes, reportedly supports broadband on gyrotrons.[4,5,11] To date, how-ever, no attempt has been made to design a mode-selective circuit for TE_{01} mode gyro-BWO.

This investigation presents a transverse sliced interaction structure for the $TE_{01}^{(1)}$ gyro-BWO. Since the wall surface current for the TE_{0n} mode is in the azimuthal direction only, the TE_{01} wave is almost unaffected as it travels through the transverse slice. In contrast, the competing modes with axial surface currents are significantly affected. Mode-selective effect is analyzed using the high-frequency structure simulator. An experiment based on this mode-selective circuit will be conducted. The $TE_{01}^{(1)}$ gyro-BWO is demonstrated to be mode-competition free and is continuously tuned over a broad range of the magnetic fields adjustments with decent efficiency. The results of this study can also be applied to other circularly symmetric electric-field mode (such as TE_{0n} modes) gyrotrons and should help in the pursuit of high-power terahertz sources.

The interaction length of the gyrotron is typically limited for stability. To elucidate the advantage of mode-selective circuit, a sufficiently long interacting structure (12.5 cm) with optimized high efficiency is adopted [Fig. 2(a)]. A steady-state, particle-tracing, self-consistent code[1] is employed to evaluate the performance of the operating mode and the starting behaviors of all potentially competing modes.
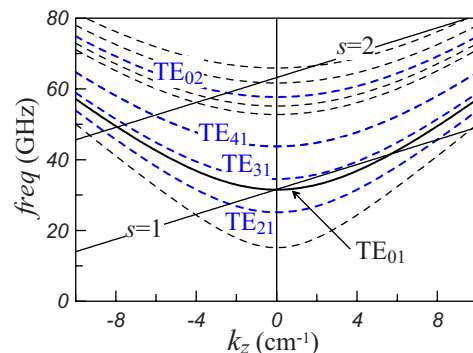

FIG. 1. (Color online) Frequency vs k_z diagrams for waveguide TE modes and beam-wave resonance lines (*s* denotes the cyclotron harmonic number). Parameters are waveguide radius (r_w)=0.58 cm, beam voltage (V_b) =100 kV, velocity ratio ($\alpha \equiv v_\perp / v_z$)=1.1, and magnetic field (B_0) =13.5 kG.

a)Electronic mail: thschang@phys.nthu.edu.tw.

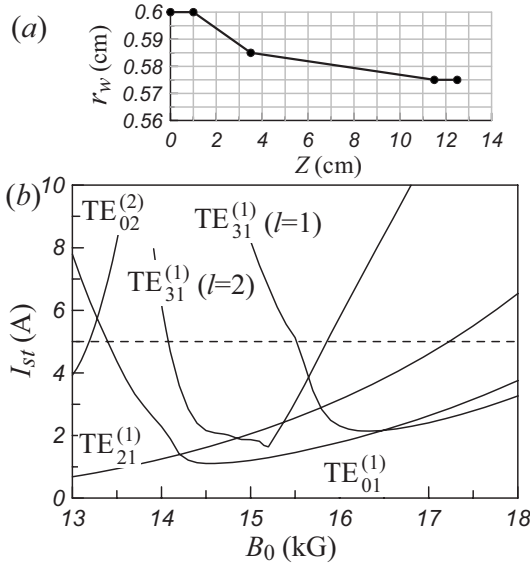**94**, 101501-1 © 2009 American Institute of Physics

FIG. 2. (a) Configuration of simulated interaction structure. (b) Start-oscillation currents vs B_0 for potentially competing modes at $V_b = 100$ kV.

FIG. 3. (Color online) (a) Transverse sliced structure. (b) Calculated loss factor vs normalized frequency (f_0/f_c) for the modes of interest, where f_c is the respective cutoff frequency ($r_w = 6$ mm, $r_s = 23$ mm, and $\Delta L = 1$ mm).

The magnetron injection gun (MIG) was developed for the $TE_{11}^{(1)}$ Ka-band experiment ($r_c = 0.09$ cm). To modify the MIG in favor of $TE_{01}^{(1)}$ interaction at Ka-band, the ordinary concentric electron beamlet is offset by a distance (r_{off}) of 0.28 cm, and thus the offset guiding center r_c' ranges from 0.19 to 0.37 cm. The velocity ratio (pitch α) of the MIG gun declines as the magnetic field increases. The relevant function is

$$\alpha = \left[(1 + \alpha_{\text{ref}}^{-2}) \left(\frac{B_0^2}{B_{\text{ref}}^2} \right) - 1 \right]^{-1/2}. \quad (1)$$

The pitch α is presumed to 1.2 (α_{ref}) at a reference magnetic field of 13 kG (B_{ref}). It decreases as B_0 increases, significantly limiting the 3 dB tuning bandwidth, as will be discussed in the experimental section.

Figure 2(b) plots the starting current (I_{st}) as a function of B_0 for all of the modes of interest. The I_{st} of $TE_{21}^{(1)}$, $TE_{31}^{(1)}$ fundamental ($l=1$) and second axial modes ($l=2$) are well below the operating current of 5 A. Moreover, the starting threshold of operating mode is higher than that of competing modes in the regions $B_0 < 14.2$ kG and $B_0 > 16.5$ kG. Without a mode-selective circuit, severe mode competitions are expected in this configuration. The dominant mode is difficult to predict from the starting behaviors and should be analyzed from start-up scenarios. Notably, the $TE_{02}^{(2)}$ mode, the most competitive mode in $TE_{01}^{(1)}$ gyro-TWT,[8] is not a threat when the system is operated at backward-wave region.

Figure 3(a) depicts the cross-sectional view of a representative structure for a single transverse slice. The copper cylindrical shell with outer radius r_s and inner (waveguide) wall radius r_w is divided into two parts and separated by a distance of ΔL. As the wave propagates through the slice, the coupling wave is induced and travels toward the terminal boundary. Either a heavy load or an open boundary can be used to terminate the coupling wave, and the latter is adopted in our system. Therefore, the coupling wave power partially diffracts into the space and is partially reflected. Multiple reflections occur between the boundaries of r_s and r_w, causing the slice to behave as an open resonator. The resonant
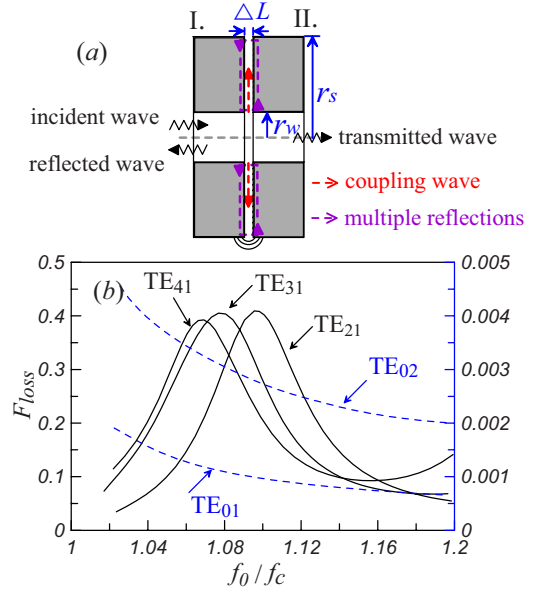
frequency depends on the reflection coefficients and the reflection loop ($r_s - r_w$). The loss factor (F_{loss}), defined as the total power loss normalized to the input power ($P_{\text{loss}}/P_{\text{in}}$), is introduced to specify the mode-selective effect. The loss factor is maximum at the resonant frequency, and the maximum values for the TE_{21}, TE_{31}, and TE_{41} modes are all about 0.4 [Fig. 3(b)], which means 40% of the wave power of a competing mode is absorbed by a single transverse slice. The loss factor for the operating TE_{01} mode is two orders of magnitude lower than those of the competing modes and is negligible. The TE_{02} has similar characteristics to the TE_{01} mode and is also less affected. Numerous transverse slices with various resonant frequencies could be combined to achieve an intensive and broadband suppression.

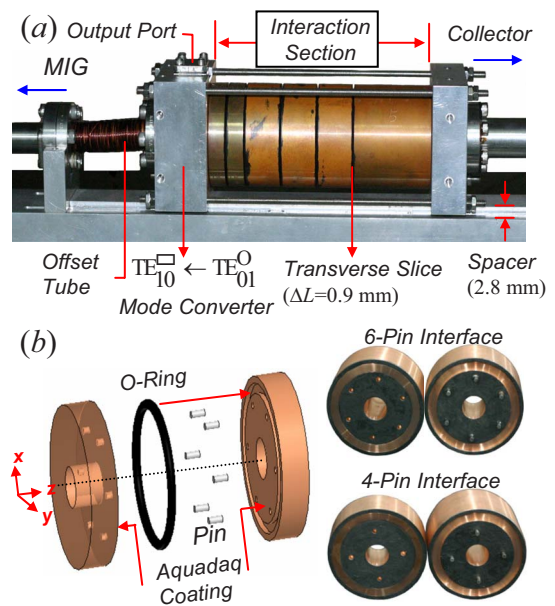Figure 4(a) displays the integrated rf structure. The elec-

FIG. 4. (Color online) (a) Integration of rf structure, (b) representative drawing, and photographs of transverse sliced structure in the experiment.
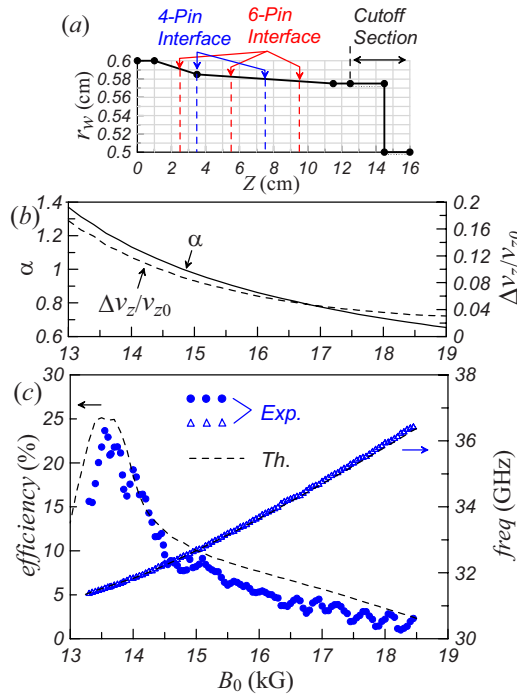
FIG. 5. (Color online) (a) Configuration of interaction structure with five transverse slices. (b) Simulated pitch α and corresponding axial velocity spread $\Delta v_z/v_{z0}$ vs B_0. (c) Experimental interacting efficiency (filled circles) and corresponding frequency (empty triangles) vs B_0 at $I_b=4.5$ A and $V_b=93.6$ kV. Theoretical predictions are shown in broken lines.

tron beam passes through an offset tube and becomes an off-axis beam in favor of $TE_{01}^{(1)}$ interaction. This tube is up-shifted by a spacer with a thickness of 2.8 mm. The whole interaction length was divided into six parts by five transverse slices. Figure 4(b) shows the design and the finished parts. The pins and corresponding holes on two connecting parts were precisely aligned. An O-ring was employed to seal the vacuum for each transverse slice. As shown in Fig. 4(b), four-pin and six-pin setups are designed better to suppress $TE_{21}^{(1)}$ and $TE_{31}^{(1)}$ modes, respectively. The generated backward wave is extracted by a high-performance Y-type TE_{01} mode converter.[12]

Figure 5(a) depicts the interaction structure with transverse slices. In comparison to Fig. 2(a), an additional cutoff section, whose sidewall is coated with heavy losses, is incorporated into the collector end. Based on MIG simulations, Fig. 5(b) plots the simulated velocity ratio and axial velocity spread as functions of magnetic field. Figure 5(c) shows the interacting efficiency and the corresponding frequency for magnetic field tuning. Both the simulations (dashed lines) and the experimental results (symbols) are displayed. The

measured peak efficiency of TE_{01} gyro-BWO with the mode-selective circuit is 23.7%, corresponding to 100 kW at 31.55 GHz, $B_0=13.55$ kG, $I_b=4.5$ A, and $V_b=93.6$ kV. An extremely wide range of continuous tuning from 31.4 to 36.4 GHz (15.8%) is achieved. The 3 dB tuning bandwidth (0.75 GHz, 2.3%) is narrow due to the decline in pitch α. The output signals, diagnosed by the oscilloscope and the spectrum analyzer, are stable and free from parasitic oscillation. As the beam power increases, however, nonstationary behaviors[2,6] were observed in a part of the tuning region. The experimental results that are shown in Fig. 5(c) agree closely with theoretical predictions.

In summary, the tunability of a TE_{01} gyro-BWO in the *Ka*-band was verified experimentally, and the high efficiency (23.7% at 100 kW output power) was demonstrated under the pulse operation (~ 1 μs). The mode-selective circuit, with the transverse sliced structure, effectively suppresses the major competing $TE_{21}^{(1)}$ and $TE_{31}^{(1)}$ modes and is harmless to operating $TE_{01}^{(1)}$ mode. This mechanism can also be applied to other gyrodevices to suppress severe mode competition.

[1]S. H. Chen, K. R. Chu, and T. H. Chang, Phys. Rev. Lett. **85**, 2633 (2000).
[2]T. H. Chang, S. H. Chen, L. R. Barnett, and K. R. Chu, Phys. Rev. Lett. **87**, 064802 (2001).
[3]S. Y. Park, R. H. Kyser, C. M. Armstrong, R. K. Parker, and V. L. Granatstein, IEEE Trans. Plasma Sci. **18**, 321 (1990).
[4]S. V. Samsonov, G. G. Denisov, V. L. Bratman, A. A. Bogdashov, M. Y. Glyavin, A. G. Luchinin, V. K. Lygin, and M. K. Thumm, IEEE Trans. Plasma Sci. **32**, 884 (2004).
[5]W. He, A. W. Cross, A. D. R. Phelps, K. Ronald, C. G. Whyte, S. V. Samsonov, V. L. Bratman, and G. G. Denisov, Appl. Phys. Lett. **89**, 091504 (2006).
[6]T. H. Chang, C. T. Fan, K. F. Pao, K. R. Chu, and S. H. Chen, Appl. Phys. Lett. **90**, 191501 (2007).
[7]K. R. Chu, Phys. Fluids **21**, 2354 (1978).
[8]H. H. Song, D. B. McDermott, Y. Hirata, L. R. Barnett, C. W. Domier, H. L. Hsu, T. H. Chang, W. C. Tsai, K. R. Chu, and N. C. Luhmann, Jr., Phys. Plasmas **11**, 2935 (2004).
[9]C. K. Chong, D. B. McDermott, and N. C. Luhmann, Jr., IEEE Trans. Plasma Sci. **26**, 500 (1998).
[10]Q. S. Wang, D. B. McDermott, and N. C. Luhmann, Jr., Phys. Rev. Lett. **75**, 4322 (1995).
[11]G. G. Denisov, V. L. Bratman, A. W. Cross, W. He, A. D. R. Phelps, K. Ronald, S. V. Samsonov, and C. G. Whyte, Phys. Rev. Lett. **81**, 5680 (1998).
[12]C. F. Yu and T. H. Chang, IEEE Trans. Microwave Theory Tech. **53**, 3794 (2005).